

# An Electrically Small Planar Antenna Using Complementary Split-Ring Resonators

Min-Da Chiou<sup>1</sup> and Shih-Yuan Chen<sup>2</sup>

<sup>1</sup> Graduate Institute of Communication Engineering, National Taiwan University  
Taipei 10617, Taiwan, [evadcmd@gmail.com](mailto:evadcmd@gmail.com)

<sup>2</sup> Department of Electrical Engineering, National Taiwan University  
Taipei 10617, Taiwan, [syichen@cc.ee.ntu.edu.tw](mailto:syichen@cc.ee.ntu.edu.tw)

## 1. Introduction

Electrically small antennas have been investigated for more than half a century, and many interesting results and structures have been obtained. Among them, the most important deduction may be the “Chu-limit,” which relates the volume occupied by an antenna to its radiation characteristics and bandwidth by introducing the concept of the quality factor. Particularly, the bandwidth-efficiency product of an antenna is limited by its electrical size [1]-[3]. The bandwidth here is defined by a specified level of reflection coefficient ( $|S_{11}|$ ) rather than the half-power bandwidth that is commonly used in the circuit theory [3]. Chu’s analysis was based on the spherical wave function expansion of fields radiated by the antenna. Since the spherical eigenfunctions are orthogonal, no energy could be coupled among modes, and therefore, each spherical mode can be represented by an individual equivalent circuit, for which the quality factor, or  $Q_{\text{mode}}$ , can be calculated. Then, the quality factor of the antenna  $Q$  can be expressed as a function of  $Q_{\text{mode}}$ ’s. Importantly, it was also shown that  $Q_{\text{mode}}$  of the lowest order mode is the lower bound for  $Q$  of a single-resonant antenna [2]. Consider the impedance bandwidth defined by  $|S_{11}| \leq -10$  dB:  $\text{BW} = \Delta f/f_0$ , where  $\Delta f$  and  $f_0$  are the absolute bandwidth and the self-resonant frequency of the antenna, respectively. Combining the results in [2] and [3] yields the upper bound for the bandwidth:  $\text{BW} \leq 1/(\sqrt{2}Q_{\text{Chu}})$ , where  $Q_{\text{Chu}} = \eta/(ka)^3$ ,  $k = \omega_0\sqrt{\mu\epsilon}$ ,  $\eta$  is the radiation efficiency, and  $a$  is the radius of the smallest sphere enclosing the antenna. Although nothing has been mentioned about the procedures to design an electrically small antenna, it does imply that such an antenna should have rotationally symmetric structure since the  $\text{TE}_{10}$  and  $\text{TM}_{10}$  modes have the lowest  $Q_{\text{mode}}$ , which correspond to the fields radiated by a short dipole and a small loop, respectively. This also explains why the geometries of many small antennas are highly symmetric [5], [6]. In this paper, the split-ring resonators (SRRs) and the complementary split-ring resonators (CSRRs) are adopted respectively to produce the fields of the  $\text{TE}_{10}$  and  $\text{TM}_{10}$  modes when self-resonating. Two planar designs of electrically small antennas are thus proposed, and the unbalanced effects on the antenna performance are discussed. Both antennas are designed to be input matched for 50  $\Omega$ , and their overall sizes are merely about  $(\lambda_0/20) \times (\lambda_0/20)$ .

## 2. Split-Ring Resonators

Since in this work, the SRRs and CSRRs are used to construct electrically small antennas, their characteristics should be briefly discussed first. The geometry of broadside-coupled SRRs are shown in Fig. 1 along with the current distribution indicated by the arrows. The two split rings of the broadside-coupled SRRs are opposite oriented such that the reverse current distribution on the rings with the open-end boundary conditions creates an inter-ring capacitance, while the narrow strips forming the rings provide the inductance. In other words, the ring itself forms a single-turn loop inductor, while the two broadside-coupled rings form a capacitor. Based on the quasi-static analysis, the capacitance taking into account the sinusoidal current distribution is derived as

$$C = \left( \frac{4 - 2\sqrt{2}}{\pi} \right) C_0 = \left( \frac{4 - 2\sqrt{2}}{\pi} \right) \left[ \epsilon_0 \epsilon_r \frac{\pi (r^2 - (r-w)^2)}{d} \right] \dots \dots (1)$$

, where the correction term in the first parentheses accounts for the sinusoidal current distribution. Also, the ring inductance  $L$  can be predicted accurately by the formula provided in [6]. Then, the self-resonant frequency of the SRRs can be obtained as

$$f_0 = \frac{1}{2\pi\sqrt{LC}} \dots \dots (2)$$

Note that these formulas are very helpful in designing electrically small antennas with SRRs/CSRRs.

### 3. Electrically Small Antenna Using SRRs

First, we propose an electrically small planar antenna using the broadside-coupled SRRs. The antenna geometry is shown in Fig. 2. To facilitate the feeding of the SRRs, the conductor-backed CPW (CBCPW) is used as the feed line, and a small half loop used as the feeding/coupling structure is protruded from the central signal trace of the CBCPW and shorting to one side of the truncated ground plane. The planar monopole topology is chosen here due to its planar structure and easy feeding by planar transmission lines, and therefore, only the upper half of the SRRs is needed in this design. Note that the resonant frequency of this antenna is determined by the self-resonant frequency of the SRRs and that the impedance matching can be adjusted simply by changing the size of the small half loop, and hence the coupling level.

A prototype antenna is designed, fabricated, and tested. It is implemented on a 31-mil Duroid 5880 substrate, and its resonant frequency calculated by (2) is at approximately 740 MHz. The simulated and measured  $|S_{11}|$  of the prototype antenna are plotted in Fig. 3, and they agree well. Both simulated and measured resonant frequencies are close to the predicted value. However, the bandwidth is surprisingly wide though the antenna size is merely  $(\lambda_0/19) \times (\lambda_0/19)$  considering only the half SRRs and their images. The reason is that the unbalanced effect of the feed line occurs since the antenna structure is not symmetric with respect to the feed line (longitudinal direction). The unbalanced currents on the bilateral ground planes inevitably contribute to the far-field radiation. Therefore, the ground plane area of the feed line should also be accounted for in the total antenna area, and this would increase the "real" antenna size, and hence the bandwidth.

### 4. Electrically Small Antenna Using CSRRs

To avoid the unbalanced effect, a novel electrically small CSRRs antenna fed by a CBCPW is proposed. Its geometry is shown in Fig. 4. The entire structure is symmetric with respect to the longitudinal direction so that the unbalanced affect could no longer occur. The square shape is adopted to suppressed the unwanted resonant modes existing between the CSRRs and the outer edges of the ground plane. In the top metallic layer, the coupled slotlines of the feeding CBCPW enter the CSRRs via the split opening and are terminated by a gap open circuit. The open-ended CBCPW itself forms a small magnetic current loop, coupling to the CSRRs. Due to the shielding of the ground planes, the radiation to the upper half space (+z) is dominated by the top ring slot of the CSRRs, while the radiation to the lower half space (-z) is dominated by the ring slot on the bottom layer. They together radiate in the whole space as a x-directed short magnetic dipole.

A prototype antenna is designed, fabricated, and tested. It is also implemented on a 31-mil Duroid 5880 substrate, and its resonant frequency calculated by (2) and duality is about 715.5 MHz. The antenna area considering only the CSRRs is merely  $(\lambda_0/22.5) \times (\lambda_0/22.5)$ . The simulated and measured  $|S_{11}|$  are plotted in Fig. 5, and they agree well. Both simulated and measured resonant frequencies are about 40 MHz higher than the predicted one (about 5% error). The simulated and measured impedance bandwidths are 0.40% and 0.33%, respectively. The radiation patterns of the prototype antenna are plotted in Fig. 6. Due to the finite size of the ground plane ( $0.3\lambda_0 \times 0.3\lambda_0$ ), which is common for practical slot radiators, the pattern nulls in the xz-plane fill up, while the yz-plane pattern, which in theory should be omni-directional, dents in the  $\pm y$  directions. Besides, the cross-polarized components in the measured patterns are increased by the scattering of the coaxial cable used for pattern measurement, which is electrically large and is of course larger than the prototype antenna. Table 1 compares the performance of our proposed CSRRs antenna to two benchmark electrically small planar antennas [4], [5]. For fair comparison, the factor  $Q/Q_{\text{Chu}}$  is considered:  $Q = 1/(\sqrt{2} \cdot \text{BW})$  and  $Q_{\text{Chu}} = \eta/(ka)^3$ , where BW represents the -10-dB bandwidth,  $a$  is the radius of the smallest sphere enclosing the antenna, and  $\eta$  is the radiation efficiency. Clearly, our proposed CSRRs antenna having a similarly small size exhibits comparable performance. From fabrication's perspective, however, our proposed design is superior to that [4] because of its

coplanar structure, and it needs no extremely narrow slots for size reduction, which is in practice difficult to realize, as required by the design of [5].

Table 1. Summary of measured results of the proposed CSRRs antenna and other benchmark planar designs.

	Antenna area	Ground plane size	Resonant frequency (MHz)	Impedance bandwidth	Radiation efficiency	$Q/Q_{Chu}$	
[4]	$\lambda_0/23.4$ in diameter	$0.4\lambda_0$ in diameter	305.2	0.16%	17%	6.12	
[5]	$\lambda_0/20 \times \lambda_0/20$	$0.5\lambda_0 \times 0.5\lambda_0$	298.8	0.33%	30%	5.52	
This work (CSRRs)	$\lambda_0/22.5$ $\times \lambda_0/22.5$	$0.3\lambda_0 \times 0.3\lambda_0$	Simulated	758.0	0.40%	24%	5.74
			Measured	756.5	0.33%	22.8%	7.50

## Acknowledgments

This work was supported by the National Science Council, Taiwan, under Contracts NSC 100-2221-E-002-237 and NSC 100-2120-M-002-009.

## References

- [1] J. Chu, "Physical limitations of omni-directional antennas," *J. Appl. Phys.*, vol. 19, pp. 1163-1175, Dec. 1948.
- [2] R. E. Collin and S. Rothschild, "Evaluation of antenna Q," *IEEE Trans. Antennas Propagat.*, vol. AP-12, pp. 23-27, Jan. 1964.
- [3] A. D. Yaghjian and S. R. Best, "Impedance, bandwidth, and Q of antennas," *IEEE Trans. Antennas Propagat.*, vol. 53, pp. 1298-1324, Apr. 2005.
- [4] O. S. Kim and O. Breinbjerg, "Miniaturised self-resonant split-ring resonator antenna" *Electron. Lett.*, vol. 45, no.4, pp. 196-197, Feb. 2009.
- [5] R. Azadegan and K. Sarabandi, "A Novel Approach for Miniaturization of Slot Antennas," *IEEE Trans. Antennas and Propagat.*, vol. 51, no. 3, Mar. 2003.
- [6] S. S. Mohan, M. del Mar Hershenson, S. P. Boyd, and T. H. Lee, "Simple Accurate Expressions for Planar Spiral Inductances," *IEEE Journal of Solid-State Circuits*, vol. 34, no. 10, Oct. 1999.

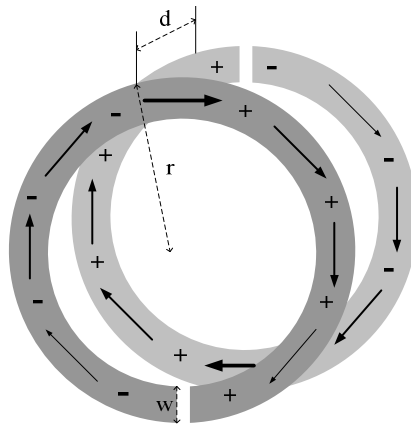


Fig. 1. Geometry of broadside coupled SRRs.

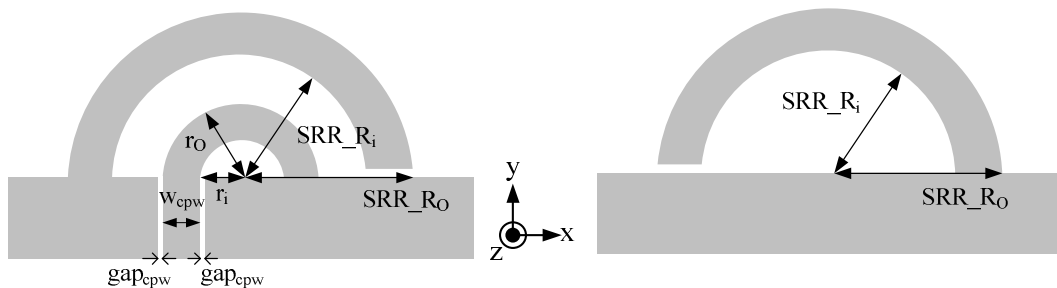


Fig. 2. Top (left) and bottom (right) views of the proposed CBCPW-fed electrically small SRRs antenna. ( $SRR_{R_0} = 10.5$  mm,  $SRR_{R_i} = 7.5$  mm,  $r_0 = 4$  mm,  $r_i = w_{cpw} = 2$  mm, and  $g_{cpw} = 0.2$  mm)

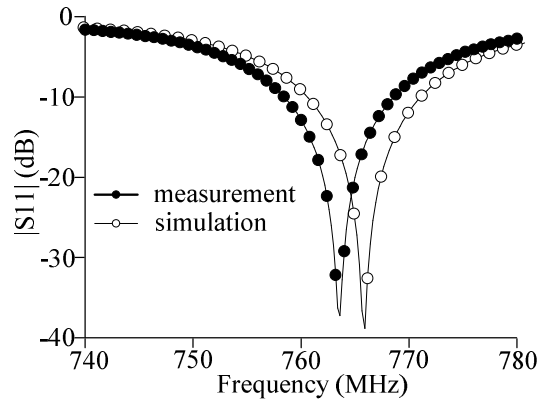


Fig. 3. Simulated and measured  $|S_{11}|$  of the proposed CBCPW-fed electrically small SRRs antenna.

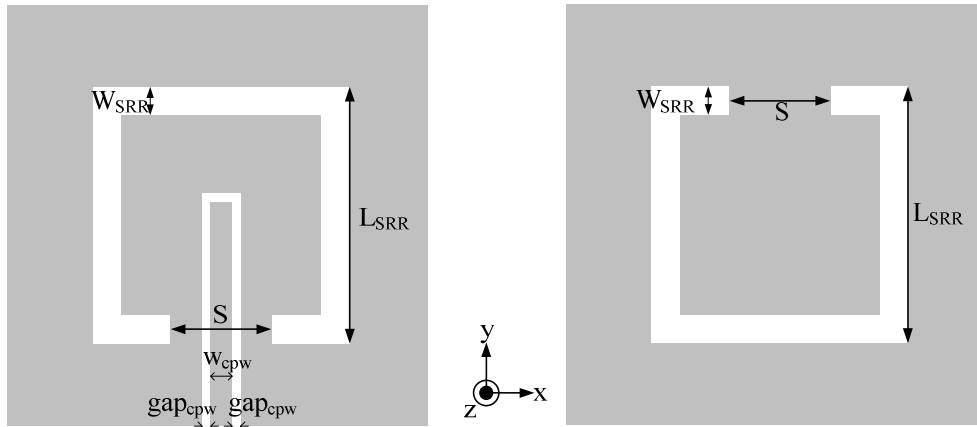


Fig. 4. Top (left) and bottom (right) views of the proposed CBCPW-fed electrically small CSRRs antenna. ( $L_{SRR} = 17.6$  mm,  $W_{SRR} = 1.5$  mm,  $S = 5.4$  mm,  $w_{cpw} = 2$  mm, and  $g_{cpw} = 0.2$  mm)

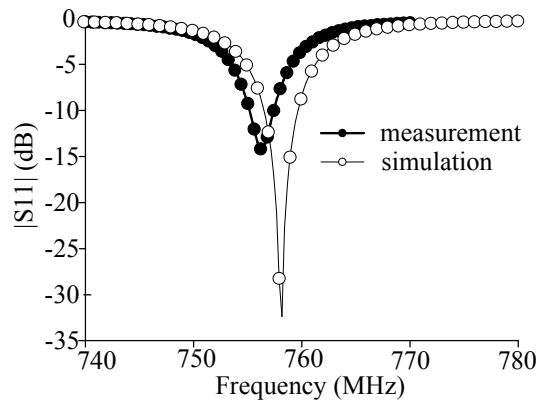


Fig. 5. Simulated and measured  $|S_{11}|$  of the proposed CBCPW-fed electrically small CSRRs antenna.

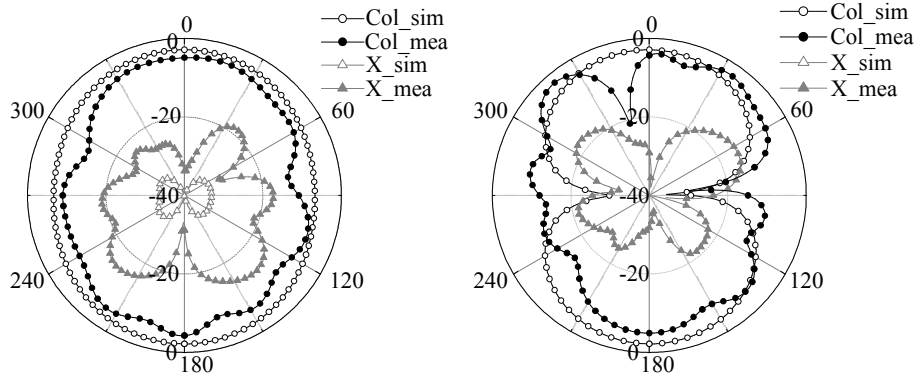


Fig. 6. xz-plane (left) and yz-plane (right) patterns of CBCPW-fed electrically small CSRRs antenna.